Available online at www.sciencedirect.com
ScienceDirect
Coordination Chemistry Reviews 252 (2008) 306–317
COORDINATION CHEMISTRY REVIEWS
www.elsevier.com/locate/ccr

Review

^{18}O-Water exchange in photosystem II: Substrate binding and intermediates of the water splitting cycle

Warwick Hillier*, Tom Wydrzynski**

Research School of Biological Sciences, The Australian National University, Canberra, ACT 0200, Australia

Received 11 April 2007; accepted 5 September 2007
Available online 11 September 2007

Contents

1. Introduction 307
2. Spectroscopic analysis of substrate water in photosystem II 307
   2.1. Vibrational spectroscopy 307
   2.2. Magnetic resonance 307
3. Analysis of substrate water exchange by mass spectrometry 308
4. Effect of the protein environment on substrate water exchange 309
5. Comparative inorganic ligand exchange processes 311
   5.1. Divalent metals 311
   5.2. Trivalent metals 312
   5.3. Manganese aqua exchange 312
   5.4. Quantum mechanical calculations of water exchange 313
   5.5. Effect of ligands and charge on aqua exchange 313
   5.6. Labilization effects on ligand exchange 313
   5.7. Bridging μ-oxo and terminal oxo exchange 314
   5.8. Calcium 315
6. Summary and overview of exchange behavior 315
7. Concluding remarks and future perspectives 316
   Acknowledgments 316
   References 316

Abstract

Photosynthetic water oxidation proceeds via four light-activated intermediate states. The nature of the substrate water in each of these intermediate states is important for understanding the mechanism of the photosynthetic O–O bond formation. Oxygen-18 water exchange measurements have been used to probe the binding of the substrate water at the water oxidation site in photosystem II. In this review we summarize the water exchange behaviour for a range of aqua-metal complexes for comparison with the Photosystem II exchange measurements. The analysis provides a basis for determining the nature of the substrate water in each of the intermediate states in the photosynthetic reaction cycle.

Keywords: Oxygen evolving complex; Photosystem II; Substrate water; Ligand exchange

Abbreviations: bpea, bis(2-pyridyl)ethylamine; bpy, 2,2′-bipyridine; cyclen, 1,4,7,10-tetraazacyclododecane; dien, diethylenetriamine; EDTA, ethylenediaminetetraacetate; en, 1,2-diaminoethane; FTIR, Fourier transform infrared spectroscopy; J–T, Jahn–Teller distortion; LFSE, ligand field stabilization energy; Me_4cyclam, *N*,*N*′,*N*″-tetramethyl-1,4,8,11-tetraazacyclotetradecane; MIMS, membrane inlet mass spectrometry; PSII, photosystem II; Terpy, 2,2′:6′,2″-terpyridine; tpy, 2,2′,2″-terpyridine; tren, 2,2′,2″-triaminotriethylamine trien triethylentetramine; trine, triethylentetramine; WOC, water oxidizing complex.

* Corresponding author. Tel.: +61 2 6125 5894; fax: +61 2 6125 8056.
** Corresponding author. Tel.: +61 2 6125 5892; fax: +61 2 6125 8056.
E-mail addresses: Warwick.Hillier@anu.edu.au (W. Hillier), Tom.Wydrzynski@anu.edu.au (T. Wydrzynski).

0010-8545/$ – see front matter © 2007 Elsevier B.V. All rights reserved.
doi:10.1016/j.ccr.2007.09.004

1. Introduction

The present atmosphere of the earth consists of 21% O_2, almost all of which has arisen from the photochemical oxidation of water by the unique pigment/protein complex called photosystem II. The annual flux of O_2 into the atmosphere is $\sim 10^{11}$ t/year and is matched by uptake reactions that almost exactly balance the production such that the net biogeochemical fluxes of production and consumption are balanced. The water oxidation reaction has been active on earth for some 2.5 GYr and the O_2 by-product has had a profound influence on the evolution of life on this planet [1,2].

The water oxidation reaction performed by PSII proceeds via a series of photoactivated intermediate states [3]. In 1970 Kok et al. [4] introduced the "S state" nomenclature to define the four stable intermediate states and one metastable state as S_n ($n = 0$–4). Only in recent years has this model been modified to take into account the proton release during the intermediates steps of the reaction [5,6]. Formally, each S-state is advanced by a light reaction that results in photochemical charge separation in the reaction center and the transfer of an oxidizing equivalent to an inorganic Mn_4Ca cluster. After four oxidizing equivalents are stored the system reacts with a consecutive 4-electron oxidation of 2 water molecules to release O_2. The structure of the catalytic site and the molecular mechanism of the S-state sequence has been the subject of considerable study through both spectroscopic and diffractive techniques (for reviews, see [7] and articles in this issue).

2. Spectroscopic analysis of substrate water in photosystem II

In many ways the nature of substrate water at the catalytic site holds the key to understanding the photochemical oxidation of water. The chemical form that the substrate takes on as it passes through the intermediate S-states is at the heart of any mechanistic model and many proposals have been advanced (for reviews see [8,9]). The substrate water interactions have been studied directly or indirectly by a variety of spectroscopic approaches that are summarized in the following sections.

2.1. Vibrational spectroscopy

One approach used to probe water in PSII is vibrational spectroscopy, which has been used to identify $^{16}O/^{18}O$ or $^{1}H/^{2}H$ sensitive vibrational modes that might be derived from the substrate water. The most widely used vibrational technique is Fourier transform infrared spectroscopy (FTIR), which has been used to investigate ν(O–H) stretching modes above 2000 cm^{-1}. Noguchi and co-workers first identified several modes in this region that were sensitive to both $^{16}O/^{18}O$ and $^{1}H/^{2}H$ exchange [10,11] and interpreted them to arise from changes manifest in H-bonding networks, or from the deprotonation of a terminal water ligand. DFT calculations of water in PSII [12] were used to substantiate these assignments. In contrast, Raman vibrational spectroscopy has been difficult to apply due to the chlorophyll and fluorescence backgrounds, yet shifted-excitation Raman difference spectroscopy (SERDS) was successfully used to identify a number of $^{1}H/^{2}H$ sensitive bending modes at low frequencies ($\sim$300–500 cm^{-1}) [13], implicating the binding of two terminal water/hydroxide molecules to the water oxidizing complex (WOC). FTIR has also been used to examine metal-oxygen bands below 1000 cm^{-1} that are sensitive to $^{16}O/^{18}O$ or $^{1}H/^{2}H$ exchange [14]. The first report of low-frequency $S_1 - S_2$ difference spectra [15] revealed a $^{16}O/^{18}O$ sensitive mode at 606 cm^{-1} that was suggested to originate from a Mn-oxo core ligand. This work was followed by detailed studies showing $^{16}O/^{18}O$ and $^{1}H/^{2}H$ sensitive modes as a function of S-state [16]. The low frequency modes reported are between 500 and 700 cm^{-1} and are strongly S-state dependent, and probably arise from bridging oxo species. This work is discussed in more detail by Noguchi (2007) in this volume.

The main limitation in the IR studies has been to directly link the vibrational modes to the substrate water. No doubt future work will couple vibrational spectroscopy with site-directed mutagenesis and high-resolution structural information to assign specific water molecules in the structure, as achieved in other systems [17].

2.2. Magnetic resonance

Magnetic resonance methods are another approach to probe the substrate water in PSII. The first experimental evidence to indicate that the Mn in PSII undergoes oxidation state changes during the O_2-evolving reaction came from the water proton NMR relaxation rate measurements at low frequencies (10–30 MHz) [18,19]. Under fast exchange conditions the effect of bound paramagnetic ions on local proton relaxation is amplified through rapid exchange with the solvent water protons. Upon flash illumination changes in the bulk paramagnetism of PSII samples could be ascribed to the bound manganese [20], which were interpreted in terms of a cycling between Mn^{3+} and Mn^{4+} at the catalytic site [21]. Although these measurements are made at room temperature where the substrate water interactions could be monitored, they are complicated by the fact that not only the protons of the substrate water contribute but also other exchangeable protons experiencing the paramagnetic effect. Measurements using EDTA indicate that the proton exchange rates in PSII samples are in the intermediate exchange condition and are influenced by protein structural changes in the PSII complex [22]. On the other hand, ^{17}O NMR relaxation rate measurements suggested that the rate of water exchange across the thylakoid membrane has to be $<10^3$ s^{-1} [19].

With the discovery of the S_2-state multi-line EPR signal at low temperatures [23], a direct probe of the catalytic Mn cluster was possible. Line broadening of the S_2 multi-line signal upon incubation of PSII samples in $H_2{}^{17}O$ indicated that water binds to the catalytic site [24]. However, when ammonia was added as a substrate analogue, the ^{17}O hyperfine interactions remained, indicating that ammonia and the water bind to different sites in the catalytic Mn cluster [25]. Subsequent ESEEM measurements confirmed a coupling between ^{17}O and the Mn [26]. Likewise, pulsed ENDOR and ESEEM measurements in the presence of D_2O have revealed strong isotropic coupling to exchangeable

deuterons [27]. Using a point dipolar approximation, quantitative analysis of the data yielded three groups of two deuterons at 2.67, 2.71 and 3.43 Å. This result was consistent with substrate water binding to the catalytic Mn in the S_2 and S_1 states [27]. Further analysis of the ESEEM measurements suggested that the first two groups of strongly coupled deuterons represent the binding of the substrate water to Mn at the catalytic site; the third group representing the weak binding of 0–10 water molecules in the outer sphere shell of the Mn cluster (∼4 Å); and a fourth group representing water bound to the protein matrix [28]. In a more recent study using proton matrix ENDOR six pairs of proton signals could be detected in both the S_0 and S_2 states [29]. Two pairs of protons were modeled as substrate water at 3.3/3.2 and 2.7 Å from the center of the Mn electron spin, based on a point dipole approximation. The different proton exchange rates that were observed in the two S states indicated that the binding affinities changed during the S-state cycle [29]. EPR studies of substrate analogues such as simple alcohols and ammonia, show that the binding of these molecules to the catalytic Mn occurs in a complex interaction with the substrate water [28,30–32].

The downside of magnetic resonance studies is the same as for the vibrational spectroscopy. The protons, deuterons and ^{17}O sites may not arise from the substrate water, but rather derive from non-substrate sites (e.g. bridging oxos) in close proximity to the metal ions. Again, with continued refinement of structural information this situation will be resolved.

3. Analysis of substrate water exchange by mass spectrometry

The most direct approach to follow water ligand exchange is via mass spectrometry. This involves the addition of ^{18}O-water and then time dependent sampling of the product. This technique has been extensively used in the field of inorganic chemistry, particularly in application to slow exchange processes [33]. With respect to PSII, substrate exchange is determined by measuring the rate of incorporation of ^{18}O from labeled water into the O_2 by-product. The O_2 generated is detected using a mass spectrometer and directly probes the substrate binding site(s). The challenge in these measurements comes in assigning the nature of the exchangeable ^{18}O species at the binding site. Early studies of ^{18}O exchange in PSII were kinetically limited to a shortest time resolution of ∼100 s [34–36] and the first time points showed that the entire substrate pool had undergone isotopic exchange. However, this approach was improved significantly with the development by Wydrzynski/Messinger and co-workers of a rapid mixing system [37] that allows the study of the exchange rates up to 175 s^{-1} (the limit imposed by mixing) [38–42]. The measurements are made using a membrane inlet mass spectrometer [43] to quantify the level of ^{18}O incorporated into the molecular oxygen generated. For these measurements, S-state populations are first preset with appropriate single-turnover flashes and dark intervals to reach the S_0, S_1, S_2 or S_3 state, into which ^{18}O-water is rapidly injected. Following progressively longer delay periods over which the lig-

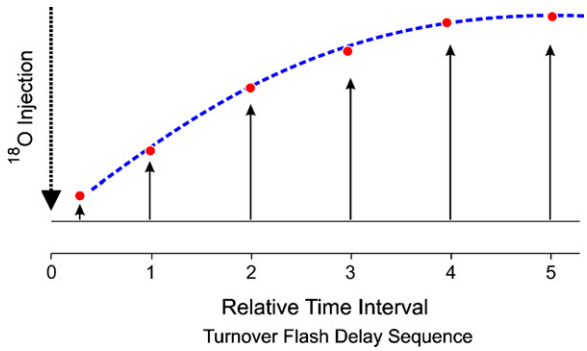

Fig. 1. The injection scheme depicted for multiple time intervals (1 → 5) and with the increasing delay times signal ultimately fully equilibrates at the final enrichment level. The spectroscopic approach is analogous to a pump-probe type spectroscopic experiment (inject – time delay – flash) from which a kinetic profile is constructed.

and exchange dynamics occurs (0.001–100 s), a flash or series of flashes is given to advance the system through the S_3–S_0 transition whereupon O_2 is released and the oxygen isotopic composition is detected by the mass spectrometer. Fig. 1 shows a scheme for the injection experiment with a curve constructed from the increasing delay times between the ^{18}O-water injection and flashes to generate the O_2. The O_2 signal ultimately increases maximally to isotopic equilibrium. The rate of increase in the ^{18}O-labeled O_2 signals show a biphasic rise at $m/e = 34$ $^{16}O^{18}O$ and a monophasic rise at $m/e = 36$ $^{18}O^{18}O$. Experimental data for spinach thylakoids at 10 °C are shown in Fig. 2. At $m/e = 36$, the $^{18,18}O_2$ signal increases mono-exponentially and can be fit with Eq. (1).

$$^{36}Y = [1 - \exp(-^{36}kt)] \quad (1)$$

At $m/e = 34$, the $^{16,18}O_2$ appears with a bi-exponential rise and can be fit with Eq. (2).

$$^{34}Y = 0.57[1 - \exp(-^{34}k_2 t)] + 0.43[1 - \exp(-^{34}k_1 t)] \quad (2)$$

The two kinetic phases at $m/e = 34$ represent the separate ^{18}O exchange rates for the two substrate water molecules. The slow phase at $m/e = 34$ data ($^{34}k_1$) yields a rate constant that is identical to that observed at $m/e = 36$ data (^{36}k), consistent with the notion that the slow exchanging substrate water is the rate determining step for the exchange of the $^{18}O^{18}O$ product. Thus far the biphasic behavior and the relative fast/slow contributions has been observed with spinach thylakoid membranes, PSII membrane fragments, and core particles including those derived from *Thermosynechococcus elongatus*. Table 1 shows a comparison of ^{18}O exchange for the S_3 state. The results show that the two phases are an intrinsic property of PSII, rather than a consequence of sample heterogeneity or sample type. In terms of kinetic modeling, the behavior appears to be well accommodated as a pseudo-first-order reaction [37,38]. The exchange rate is thus a measure of the time for each site to reach isotopic equilibration, which will be the rate determining process for the corresponding dissociation/association of the H_2O ligand at its binding site.

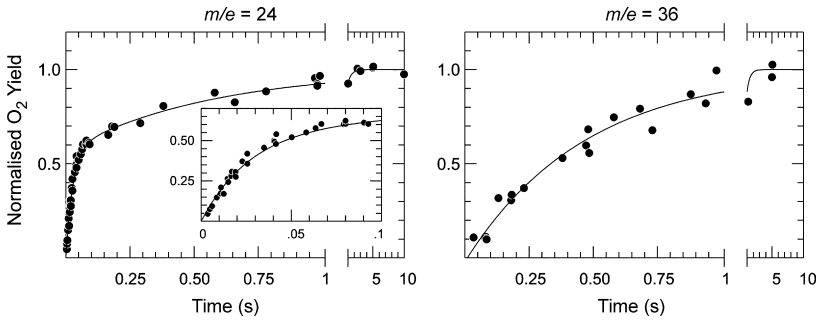

Fig. 2. The normalized yields of O_2 produced on the third flash by spinach thylakoid samples plotted as a function of $H_2{}^{18}O$ incubation time, in the S_3 state. Measurements were made at $m/e = 34$ (left) for the mixed labeled $^{16,18}O_2$ and at $m/e = 36$ (right) for the double labeled $^{18,18}O_2$ at 10 °C. Solid lines show first-order kinetic fits from Eqs. (1) and (2). The rate constants of $38 \pm 2\,s^{-1}$ for the fast phase and $1.8 \pm 0.2\,s^{-1}$ for the slow phase were obtained. Further details can be found in [45].

Table 1
Rate constants for ^{18}O exchange in the S_3 state of different PSII samples

Sample (10 °C)	$^{34}k_1$ (s^{-1})	$^{34}k_2$ (s^{-1})
Thylakoid membranes (*Spinacia*) (H_2O)	1.8 ± 0.2	38.0 ± 2.0
Thylakoid membranes (*Spinacia*) (D_2O)	1.9 ± 0.2	52.0 ± 2.1
Thylakoid membranes (*Synechocystis*)	3.8 ± 1.3	25.9 ± 6.7
PSII membrane fragments (*Spinacia*)	2.1 ± 0.1	37.3 ± 1.6
Ca^{2+}-depleted PSII with $CaCl_2$	1.4 ± 0.1	27 ± 2
Ca^{2+}-depleted PSII with $SrCl_2$	5.2 ± 1.7	23 ± 5
Minus 16 and 23 kDa extrinsics	1.7 ± 0.3	22.7 ± 2.0
Minus 16, 23 and 33 kDa extrinsics	1.6 ± 0.7	9.7 ± 2.6
PSII core particles (*Spinacia*)	1.1 ± 0.4	18.0 ± 3.9
PSII core particles (*T. elongatus*)	0.5 ± 0.1	34.6 ± 2.3
PSII core particles (*Synechocystis*)	0.9 ± 0.2	15.2 ± 2.4

Data from [40,42].

The signal for the $^{16}O^{16}O$ species can be measured at $m/e = 32$ and by using the three O_2 isotopic products ($m/e = 32$, 34, 36) the enrichment can be determined. The equilibrium O_2 values are to within ±0.2% of those expected for the ^{18}O enrichment (ε) when the oxygen signals are measured simultaneously.

$$32 : 34 : 36 = (1 - \varepsilon)^2 : 2(1 - \varepsilon)\varepsilon : \varepsilon^2 \quad (3)$$

The first experiments using this technique established the ^{18}O exchange behavior for the two substrate water molecules in the S_3 state [37,38]. Subsequently the entire S-state dependence [39], the involvement of Ca^{2+} [42] and the role of the extrinsic proteins [40] in the exchange process were determined. In Table 2 the S-state dependence of the exchange rates for spinach thylakoids (10 °C, pH 6.8) is given. The results reveal that one substrate water molecule is resolvable in each S state (S_0 to S_3) while the second substrate water molecule is resolvable only in the S_2 and S_3 states. The two substrate water molecules do not exhibit interconversion between sites 1 and 2, because the relatively long delay times between the turnover flashes (3 or 5 ms) used to generate O_2 (e.g. S_1 is given three flashes after ^{18}O water injection) would allow significant exchange of fast water to occur and perturb the ratio of fast:slow in Eq. (2). This is not observed. The S-state dependence thus shows that the slow site in S_0 exchange is more tightly bound by 500× in S_1, is less tightly bound by 100× in S_2 and remains unchanged in the S_3 state. In contrast, the unresolvable fast exchanging water in S_0 or S_1 appears in S_2 indicating an unquantified increase in the binding affinity, which then increases a further by 3× fold upon entering the S_3 state. These results are surprising as the exchange rates are entirely independent of each other with the two sites sharing no common behavior. This data along with activation and thermodynamic analysis [39,44,45], supports the conclusion that the two water binding sites in PSII are inequivalent throughout the reaction cycle and therefore reside at two different binding sites. A summary of the data is as follows:

Table 2
^{18}O exchange rates for thylakoid membranes from spinach as a function of S-state at 10 °C

	Substrate #1, k_1 (s^{-1})	Substrate #2, k_2 (s^{-1})
S_0	~10	–
S_1	~0.02	>120
S_2	~2.0	~120
S_3	~2.0	~40

Data from [39,45].

- The two sites are non-equivalent throughout the S-state cycle in terms of the rate of exchange, activation energy and entropy.
- The substrate water at the fast exchange site is sequentially bound more tightly after $S_1 \rightarrow S_2 \rightarrow S_3$ transitions.
- The substrate water at the slow exchange site is bound more weakly after the $S_1 \rightarrow S_2$ transition but is unchanged during $S_2 \rightarrow S_3$ transition.
- The slow exchange site binds water with remarkably similar affinity in the S_0 and final S_3 state.

We will come back to discuss these points further after we cover some of the details of water ligand exchange processes.

4. Effect of the protein environment on substrate water exchange

Solvent water most likely has access to the catalytic site in PSII via the lumenal side of the thylakoid vesicle and thus must cross the membrane as well as any protein barrier formed by the PSII complex. The rate of water transport across the thylakoid membrane to the lumen is estimated to be $\sim 10^{-3}\,s^{-1}$

[19]. Since the resolvable ^{18}O exchange rates are slower than this rate, it appears that ^{18}O isotope exchange is not limited by water transport across the membrane. This is confirmed by measurements of PSII membrane fragments and core preparations which have similar rates of ^{18}O exchange compared with intact thylakoid vesicles [40]. Since the catalytic site is situated towards the interior of the PSII complex, there could be a protein barrier which influences the rates of ^{18}O exchange. Earlier it was proposed that a restricted access of the solvent water through a protein channel to the catalytic site is a fundamental requirement for the ordered binding of the substrate water and the formation of the O–O bond [46].

A special class of proteins called aquaporins are now well-known to facilitate water transport by forming a restricted water channel [47]. The aquaporins can transport water with a high osmotic permeability ($\sim$0.02 cm s^{-1}) and low activation energies ($\sim$13 kJ mol^{-1}) compared to un-catalyzed diffusion [48]. An aquaporin protein with a channel 40 Å long can transport a water molecule in $\sim$20 μs. This rate is clearly much faster than those measured in PSII. Numerous aquaporins have been identified in plants cells and mitochondria [49] but none have been localized to the thylakoids [47]. It is clear from the literature that none of the PSII protein subunits display any of the structural/functional features characteristic of the classical aquaporins [47]. Nevertheless, there could be a directed transport of solvent water through the PSII protein matrix, which could give rise to the slow phase in ^{18}O exchanger measurements. It was suggested that the PsbO protein, which stabilizes the catalytic Mn cluster and optimizes O_2 evolution, may be the site for a water channel since it contains a high proportion of hydrophobic β-sheet structure [46]. However, ^{18}O exchange measurements of PSII samples in which the PsbO protein was biochemically removed did not show any significant increase in the exchange rates in the S_3 state, implying this was not a limiting kinetic property [40]. Similarly, ESEEM measurements of the proton couplings with the catalytic Mn in the S_1 state did not reveal any significant differences in PsbO-depleted samples [50]. However, it may be possible that excess Ca^{2+} added for activity results in subtle conformational changes in PSII that re-creates a kinetic protein barrier previously formed by the PsbO protein.

With the atomic structural information currently available on PSII, it is now possible to use cavity-searching algorithms to evaluate the existence of possible conduits in the protein matrix that could transport water molecules or O_2. Recently, the cavity program CAVER [51] was applied to the 1S5L.pdb data set [52] to identify possible passageways through connecting clefts, cavities and pockets in the PSII protein structure [53]. The analysis of the 3.5 Å structure of PSII identified three different passageways in the PSII complex having a minimal radius of 1.4 Å (which is large enough to allow water and oxygen molecules to pass) [53] (see Fig. 3). Channel (i) led from the water-splitting site to the lumen of the thylakoid vesicle following a path along the luminal surface of the CP43 subunit. The section of the channel near the water-splitting site is quite polar but gradually becomes highly hydrophobic before it exits into the lumen. Based on a comparison with a CAVER analysis of the cytochrome *c* oxidase, where a distinct O_2 channel has been identified [54–56], the authors conclude that channel (i) in PSII is a potential oxygen channel. The other two channels are more polar throughout their length,

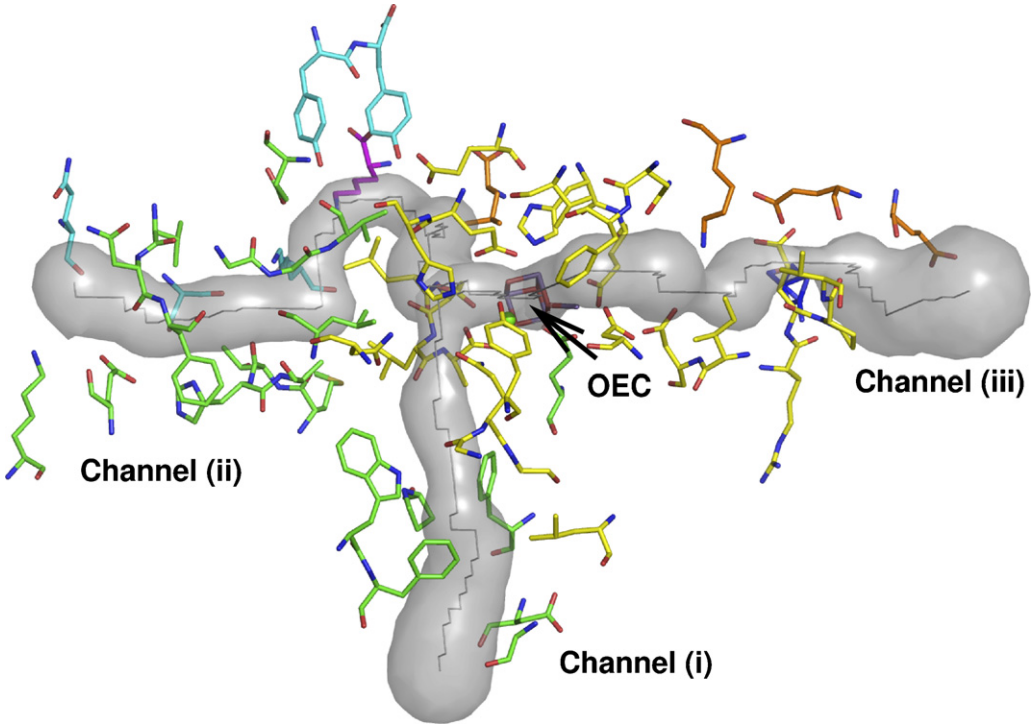

Fig. 3. Model of water and hydrophobic oxygen channels that are proposed to lead to the catalytic Mn_4Ca cluster of PSII. Figure kindly provided by Murray and Barber [53]. Channel I was proposed to be a likely O_2 channel and channels II and III possible substrate water and proton channels.

with channel (iii) being the most hydrophilic and identifiable with the channel proposed earlier by Ferreira et al. [52] to be a H^+ exit channel. Both channels (ii) and (iii) potentially shuttle H^+ and water back and forth between the exterior solvent water and the catalytic site.

The proposed channels postulated from the atomic structure of PSII probably only show one conformation that was fixed in place upon crystallization of the PSII complex. It has been argued from computational analysis of protein dynamics that a hydrophobic gas molecule such as O_2 could diffuse through pre-existing cavities or packing defects that fluctuate under physiological conditions so that there is no one set pathway [57,58]. On the other hand, it has been shown that CO_2 and NH_3 gas can be specifically transported by aquaporins [59,60] thus having a well-defined pathway through the protein. The catalytic site in PSII may have adopted some of the features of water transport to facilitate the water oxidation process.

5. Comparative inorganic ligand exchange processes

The aqua/ligand exchange literature is an active area of chemical investigation that began in the 1950–1960s [61–63] and continues today [33,64–67]. Water exchange rates of inorganic complexes span over a remarkable kinetic time scale of 20 orders of magnitude, from the exchange processes occurring in sub-nanoseconds for Eu^{3+} and Cs^{2+} complexes ($k_{ex} \approx 10^{10}\ s^{-1}$) to exchange processes occurring over >200 years for Ir^{3+} ($k_{ex} \approx 10^{-10}\ s^{-1}$). This extraordinary range is brought about by properties of the metal ions that are attributed to: (1) the size of the metal ions (ionic radii: r_M); (2) the effective magnitude of the cationic charge (Z); and (3) any ligand field stabilization energy (LFSE) associated with transition metal coordination. These parameters are summarized for Mn in Table 3. As such, the absolute rate of ligand exchange is a complex phenomenon and is not determined by a single property. These parameters (size, charge, ligand field) are also modulated in the biological context by: (1) activation barriers that are coupled to H-bonding networks; (2) modulation of the charge by the dielectric environment around the catalytic site (Bohr effect); (3) solvent levels in the second hydration (solvation) sphere; and (4) bulk solvent exchange and entry into the protein. Further constraints include the nature of the substrate in photosystem II; i.e. aqua versus hydroxo versus bridging oxo (hydroxo) versus terminal oxo. Thus, prediction of exchange rate behavior is a very difficult task. There is also no mathematical formalism that empirically relates these properties to a given exchange rate for a particular metal ion. However, given the wealth of literature on water exchange and the relative S-state dependent behavior, we will give an overview of what the ^{18}O exchange rates in PSII may be indicative.

Table 3
Electronic and structural properties of manganese ions at given oxidation states

	Mn^{II}, d^5	Mn^{III}, d^4	Mn^{IV}, d^3
LFSE $(\Delta_o)^{H\text{-}S}$	0	−0.6	−1.2
LFSE $(\Delta_o)^{L\text{-}S}$	−2.0	−1.6	−1.2
Preferred coordination	6	$6^{H\text{-}S}$ or 5	6
Lewis acidity	Strong	Strong	Very strong
Effective ionic radii r_M (pm)[a]	67	65	39
Aqua exchange (s^{-1})[a]	2×10^7	n.d.	n.d.

[a] Exchange rates from [65], and ionic radii from Appendix 3 in [65].

Any comparison of PSII with inorganic compounds is complicated by the property of Mn in solution. The higher oxidation Mn^{III} and Mn^{IV} states that are predicted for intermediates at the WOC site in PSII exhibit elevated redox potentials that have, with one exception, prevented ligand exchange measurements of model compounds. As such, the water exchange rates have only been experimentally determined for Mn^{2+}. Table 3 summarizes a number of properties of Mn ions. One complicating factor is any uncertainty in the coordination geometry of the Mn ions, which will have a large influence. However, with the continual structural refinement of PSII [52,68,69] the natural ligands to the Mn cluster have been narrowed down to a series of carboxylate and histidine residues [70]. All of the oxygen ligands to the Mn cluster (RCO_2^-, OH-, μ-oxo, H_2O) fall into the class of hard base donors that are not strongly polarized. These hard ligands tend to stabilize the coordination of the tetranuclear Mn cluster and maintain the reactivity to drive the thermodynamically difficult water oxidation reaction.

5.1. Divalent metals

The water exchange rates for the hexaaqua complexes of the divalent, first row transition metals follow the series: $Cu^{2+} > Mn^{2+} > Fe^{2+} > Co^{2+} > Ni^{2+} > V^{2+}$, as shown in Fig. 4 and Table 4. The rates span 8 orders of magnitude and are attributed primarily to differences in the electronic occupancy of the d-orbital, since charge and ionic radii are relatively unchanged across the series. The aqua exchange rates track with the high-spin ligand field stabilization energy (LFSE), as shown in the lower part of Fig. 4. As the d-shell is filled across the first

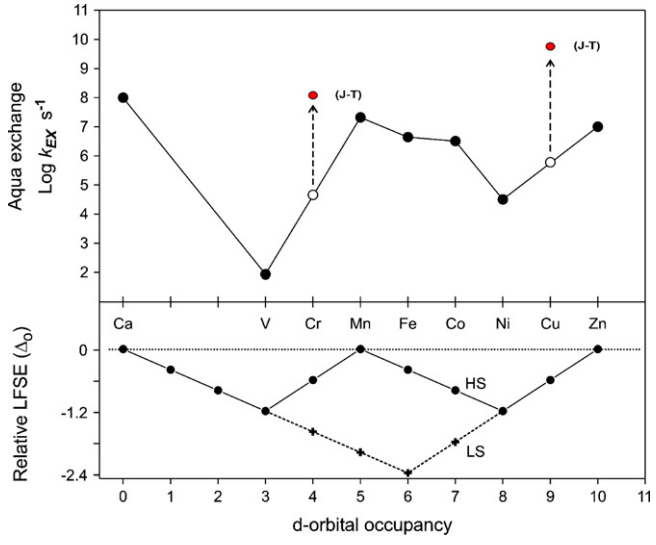

Fig. 4. Comparison of the rates of aqua exchange for the first row of the transition metal cations $[M^{2+}(H_2O)_6]^{2+}$. The Cr and Cu examples have greatly labilized aqua exchange rates due to Jahn–Teller distortions (J–T). The ligand field stabilization energy (LFSE) is presented in the lower figure for the corresponding high-spin and low-spin complexes. Figure adapted from Ref. [33].

Table 4
Water exchange rates for divalent metal aqua ions

	k_{ex} (s^{-1})[a]	r_M (pm)[a]	d-Electrons	Electronic configuration
$[Ca(H_2O)_6]^{2+}$	$\sim 1 \times 10^8$	100[b]	d^0	
$[Sr(H_2O)_6]^{2+}$	$\sim 1 \times 10^9$	118[b]	d^0	
$[V(H_2O)_6]^{2+}$	8.7×10^1	79	d^3	t_{2g}^3
$[Cr(H_2O)_6]^{2+}$	1.2×10^8	80	d^4	$t_{2g}^3 e_g^1$
$[Mn(H_2O)_6]^{2+}$	2.1×10^7	67	d^5	$t_{2g}^3 e_g^2$
$[Fe(H_2O)_6]^{2+}$	4.4×10^6	65, 55[c]	d^6	$t_{2g}^4 e_g^2$
$[Co(H_2O)_6]^{2+}$	3.2×10^6	61, 55[c]	d^7	$t_{2g}^5 e_g^2$
$[Ni(H_2O)_6]^{2+}$	3.2×10^4	69	d^8	$t_{2g}^6 e_g^2$
$[Cu(H_2O)_6]^{2+}$	5.7×10^9	73	d^9	$t_{2g}^6 e_g^3$
$[Zn(H_2O)_6]^{2+}$	$\sim 1 \times 10^7$	74	d^{10}	$t_{2g}^6 e_g^4$

[a] Exchange rates from [33,65,66], and ionic radii from Appendix 3 in [65].
[b] 6-coordinate species.
[c] High-spin vs. low-spin.

transition row ($d^2 \rightarrow d^{10}$), the d-orbital electrons become more polarizable and the exchange mechanism switches from dissociative exchange to associative exchange [33,66].

Two exceptions in this series are the hexaaquoacomplexes of Cr^{2+} and Cu^{2+}, which correspond to d^4 and d^9 electronic configurations, respectively. These ions are considerably more labile due to the Jahn–Teller (J–T) distortion in which the axial d_{z^2} bonds are lengthened (and the equatorial bonds contract). The J–T distortion can also be a property of a Mn^{3+} ion in octahedral coordination. In a recent study of this phenomenon, a series of the d^9 Cu^{2+} complexes were structurally constrained by a single 5-coordinated organic ligand in which the remaining single aqua ligand could be resolved. It was found that the Cu-complexes had either significantly reduced or entirely lost the J–T distortions and that the exchange of the aqua ligand was significantly slowed compared to hexaaquo Cu^{2+} complex [71]. Fig. 4 shows the comparable water exchange rates under non J–T conditions for the other aqua-metal complexes. The comparison shows a slower exchange rate by about 2–3 orders of magnitude when the J–T effect is suppressed.

5.2. Trivalent metals

There are several examples in the literature of aqua exchange on trivalent metal ions, although the range of rate constants is not as large as in the divalent ions because of their increased reactivity. The examples that are given in Table 5 show that water exchange is markedly slower in the trivalent metal ions compared to the divalent metal ions. Comparison of the water exchange rates for Fe^{2+}/Fe^{3+} and Ru^{2+}/Ru^{3+} hexaaqua species $[M(H_2O)_6]^{n+}$ (Tables 4 and 5) qualitatively indicate that an increase in the oxidation state of a metal ion will slow the exchange rate by a factor of ~4 orders of magnitude. The Fe and Ru examples represent d^6 and d^5 configurations, respectively, without J–T ligand distortions. The general message from these examples is that as the metal ion becomes oxidized, there is a slowing in the aqua ligand exchange rate due to the overall higher charge to r_M ratio.

Table 5
Water exchange rates for trivalent metal aqua ions

Trivalent ion	k_{ex} (s^{-1})[a]	Mono-deprotonated	k_{ex} (s^{-1})[a]
$[V(H_2O)_6]^{3+}$	5.0×10^2		
$[Cr(H_2O)_6]^{3+}$	2.4×10^{-6}	$[Cr(H_2O)_5OH]^{2+}$	1.8×10^{-4}
$[Fe(H_2O)_6]^{3+}$	1.6×10^2	$[Fe(H_2O)_5OH]^{2+}$	1.2×10^5
$[Ru(H_2O)_6]^{3+}$	2.4×10^{-6}	$[Ru(H_2O)_5OH]^{2+}$	5.9×10^{-4}
$[Rh(H_2O)_6]^{3+}$	2.2×10^{-9}	$[Rh(H_2O)_5OH]^{2+}$	4.2×10^{-5}
$[Ir(H_2O)_6]^{3+}$	1.1×10^{-10}	$[Ir(H_2O)_5OH]^{2+}$	5.6×10^{-7}

[a] Exchange rates from [33,65,66], and ionic radii from Appendix 3 in [33].

5.3. Manganese aqua exchange

The Mn ions in the WOC certainly take on the II, III, IV oxidation states and may transiently reach Mn(V). Ordinarily this ramping of oxidation state would be expected to show a profound slowing in the water exchange rates. The $[Mn(H_2O)_6]^{2+}$ ion undergoes exchange with a rate $k_{ex} = 2.1 \times 10^7\ s^{-1}$ [72]. If a similar Mn^{2+} aqua complex existed in PSII, the rate of exchange would be too fast to be resolved by the mass spec technique which is kinetically limited by ^{18}O mixing (i.e. $175\ s^{-1}$). The fast unresolved phase in S_0 and S_1 could potentially be attributed to the Mn^{2+} oxidation state, but recent work dismisses this as an oxidation state in the S_0 state [73,74].

There are no experimentally determined rates for Mn^{3+} aqua complexes but they would be predicted to have a much slower rate of exchange than Mn^{2+} aqua complexes. However, the d^4 electronic occupancy of Mn^{3+} in an octahedral field would result in a J–T distorted geometry such that axially bound water would be considerably more labile than equatorially bound water. One study using computational DFT derived estimates of metal–oxygen bond lengths made a comparison of bond length versus exchange rate and predicted a relative rate of $k_{ex} \approx 1$–$10\ s^{-1}$ for $[Mn(H_2O)_6]^{3+}$ [75].

Similarly, aqua ligands to the Mn^{4+} ion would be expected to be less exchange labile than the Mn^{3+} ion. The ionic radius of the Mn^{4+} ion is smaller (Table 3) and the d^3 electronic configurations of d_{xz}, d_{xy}, d_{yz} orbitals align between the σ-bonds to act to effectively repel incoming ligands. The relative inertness of a d^3 ion is seen in Fig. 4 for V^{2+}. Unfortunately, as stated earlier there is not a wealth of information terminal aqua exchange on Mn ions. However, in the studies of the oxo exchange in a series of $[(Terpy)(H_2O)Mn^{4+}(\mu\text{-oxo})_2Mn^{4+}(OH_2)(Terpy)]^{4+}$ compounds [76,77] the authors noted that during ESI mass spectroscopy the terminal waters are replaced with anions. In unpublished work (Gary Brudvig, *personal communication*) the authors also observed rapid anion exchange with terminal water (i.e. <5 s) indicating that the terminal sites are quite labile and that terminal exchange from Mn^{4+} is a mechanistically possible intermediate in the WOC, in contrast to we inferred earlier [78]. One caveat, however, is that the Terpy ligand set is comprised of N-donor ligands to the Mn which in turn are better at donating σ-bonds than oxygen ligands and are possibly a contributing factor to the lability of this particular aqua complex. In future studies of Mn aqua exchange it would be desirable to kinetically resolve terminal water exchange to provide further mechanistic constraints for the ^{18}O exchange results of PSII.

The general expectation for the magnitudes of water exchange rates for Mn complexes is: $Mn^{2+} > Mn^{3+} > Mn^{4+}$. Since a greater proportion of the charge is distributed onto the ligands as the oxidation state increases, the bonds shorten and the binding strengthens. The ligand exchange behavior for Mn is critical for the charge accumulation in the WOC where the Mn cluster takes on predominately higher oxidation states. The water exchange behavior in the WOC is most likely modified by the protein environment as the S-state transitions are more-or-less electroneutral (the $S_1 \rightarrow S_2$ transition aside) [8]. The oxidation state composition of the Mn cluster in PSII is discussed further in the following sections.

5.4. Quantum mechanical calculations of water exchange

Using quantum mechanical calculations the thermodynamic barriers for ligand exchange have been modeled [79] creating a renaissance in ligand exchange studies. This approach has predicted that the Mn^{2+} ion undergoes water exchange via an associative mechanism with a thermodynamic barrier of $\Delta E^{\ddagger} = 30.9\,kJ\,mol^{-1}$ while the Mn^{3+} water exchange proceeds via a dissociative mechanism with $\Delta E^{\ddagger} \sim 54\,kJ\,mol^{-1}$ [80]. Although water exchange of Mn^{3+} complexes has never been measured, the experimental values for Mn^{2+} [$\Delta H^{\ddagger} = 32.9\,kJ\,mol^{-1}$ and rate $k_{ex} = 2.1 \times 10^7\,s^{-1}$] compare well to the calculated barrier [72]. A series of model Mn^{4+} complexes have also been examined by Siegbahn and coworkers using computational approaches and provide a valuable comparative data set [81]. When operating under the premise of a charge neutral system, the $[Mn^{4+}(H_2O)_2(OH)_4]$ aqua exchange underwent a dissociative mechanism over a barrier of $\Delta E^{\ddagger} = 40.1\,kJ\,mol^{-1}$ and that of $[Mn^{4+}(H_2O)_2(OH)_3Cl]$ over a barrier of $\Delta E^{\ddagger} = 45.2\,kJ\,mol^{-1}$. The exchange of OH in the last example had a barrier of $\Delta E^{\ddagger} = 56.9\,kJ\,mol^{-1}$. One of the interesting points to come out of this study was that the Mn^{4+} aqua ion underwent exchange with a lower barrier than the exchange for the Mn^{3+} aqua mentioned above, which was due to their assessment of charge.

Energy barriers can also be related to a reaction rate for a unimolecular reaction. The basic premise in this analysis is that the faster the exchange process, the lower the energy barrier. Using the Arrhenius expression it is possible to provide an estimate of the exchange rate when the activation energy is known,

$$k_{ex} = A \exp\left(-\frac{\Delta E_A^{\ddagger}}{RT}\right) \quad (4)$$

In this application the pre-exponential term, A, is often approximated as $10^{11}\,s^{-1}$. However the Arrhenius pre-exponential term is temperature dependent and contains contributions from zero point energies, solvent interactions and entropy. In practice the A term is often found to lie between 10^{10} and $10^{16}\,s^{-1}$.

Another theoretical approach to study ligand exchange is transition state theory where:

$$k_{ex} = \frac{k_B T}{h} \exp\left(\frac{\Delta G^{\ddagger}}{RT}\right) \quad (5)$$

when the entropic and enthalpic contributions are known. This theory was employed to predict aqua exchange rates of $k_{ex} \sim 6 \times 10^5\,s^{-1}$ for $[Mn^{4+}(H_2O)_2(OH)_4]$ [81]. These types of calculations which include entropic contributions are extremely valuable for comparison with PSII.

5.5. Effect of ligands and charge on aqua exchange

Comparisons between trivalent metal ions of the type $[X(H_2O)_6]^{3+}$ with the corresponding mono-deprotonated metal ion $[X(H_2O)_5OH]^{2+}$ illustrates the effect of charge in inorganic metal complexes. The deprotonation of a single water to a hydroxo ligand both reduces the overall charge[1] on the complex and increases the corresponding water ligand exchange rates. In Table 5 rates are given for a number of examples for comparison. The mono-deprotonated metal complex shows an increase in the water ligand exchange of about 3 orders of magnitude compared with the hexa-aqua complex. This qualitative comparison is similar to the one between divalent and trivalent metal ions, where the –OH anion decreases the overall charge.

Another interesting comparison comes from a series of aqua $Ni^{2+}(d^8$ ion) complexes where the exchange rates get slower as the hydration level is decreased from $6 \rightarrow 1$ due to the presence of spectator (non-leaving) ligands. Fig. 5 shows the effect of increasing the number of the spectator ligands in the aqua Ni^{2+} series. The trend is for an increase in aqua exchange as the coordination of the spectator ligands increase. This effect however, is associated primarily with changes in bonding character, and not with heterogeneous populations or exchange mechanisms. The aqua exchange rates increase because the aqua ligands are replaced with stronger σ-donating nitrogen ligands, which in turn reduce the overall metal charge by providing electron density. There is also the competing effect from π-acceptor ligands, typically aromatics that reduce electron density on the metal and neutralize the overall σ-donating effect [65,66,82]. In terms of PSII, the effect of replacing aqua ligands with bridging oxo groups and carboxylate ligands will be moderate as the relative σ-donation of the donor ligands is similar and the change in p-orbitals will slightly increase π-acceptor characteristics.

5.6. Labilization effects on ligand exchange

Ligand exchange is influenced by the so-called ligand *trans effects*. In general, the *trans effect* is strictly a kinetic phenomenon[2] and only affects *trans* ligands on the metal binding site. The *trans effect* is strongly apparent in square planar systems but is also manifested in octahedral systems and di-μ-oxo bridging systems [33,83–85]. The labilization is due to the electronic orbital having two phases, where one phase is

[1] Mechanistically it has also been put forward that there is a specific "conjugate base" labilizing effect arising from the hydroxide group that stabilizes the transition state via π electron donation, and is potentially highly stereo specific. Further discussion can be found in [33,65].

[2] The *trans effect* should not be confused with a *trans influence* which has a thermodynamic origin. The *trans effect* also may not necessarily accompany a change in bond lengths.

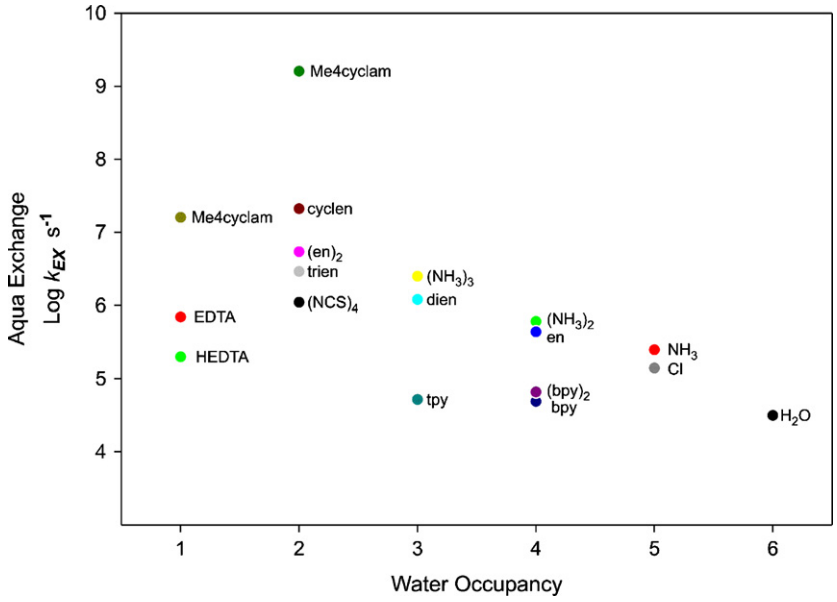

Fig. 5. Rates of water exchange for a series of Ni^{2+} complexes with varying numbers of water ligands. The ligand exchange rates then are modulated due to changes in bonding as discussed in the text.

involved in coordination of a ligand and the other phase is in the *trans* position. The *trans effect* is strongest with strong σ-donors and π-donors, e.g. $Cl^- > OH^- > OH_2$. In the examples of the Rh and Cr dimers, the bridging –OH– groups have about a 10-fold labilization on *trans* water ligands [83–85]. There does not yet appear to be any information on *trans effects* arising from bridging oxos, but given that the oxo bridges are likely to be stronger π-donors than a hydroxo, the oxo will likely exert a slightly stronger labilization effect on exchanging ligands than hydroxo.

5.7. Bridging μ-oxo and terminal oxo exchange

As we discussed above, there are a number of examples of dimeric metal complexes containing bridging μ-oxo groups. The oxygen ligand exchange for some of these metal dimers is shown in Table 6. These ligand exchange process are particularly relevant to PSII since the tetranuclear Mn cluster is known to be organized by bridging bis μ-oxo ligands. The most recent EXAFS interpretations suggest that there are 4 bis μ-oxo bridges in the Mn cluster [69]. In some proposals an oxo bridge has been predicted to be an intermediate in the water oxidation reaction [86].

The exchange of bridging di μ-oxo ligands has been measured for Cr, Rh, and Mo complexes and is summarized in Table 6. The rates are typically less than 10^{-4} s^{-1}, and have thermodynamic barriers ($\Delta H^{\ddagger}$) that can be 100 kJ mol^{-1} or more (since the oxygen ligand exchange is kinetically impeded by a rate determining ring-opening step). For model dimeric Mn complexes it was known that the di-μ-oxo ligands are exchangeable [87,88] but until recently the rates were indeterminate. However, Brudvig and co-workers [76] have in the past year measured the exchange rates for a series of Mn^{3+}/Mn^{4+} and Mn^{4+}/Mn^{4+} complexes (see Table 6). The oxo exchange rates for the mixed valence Mn^{3+}/Mn^{4+}complexes are more labile than the corresponding Mn^{4+}/Mn^{4+} species, a property attributed to the relative inert behavior of a d^3 octahedral Mn^{4+} ion [76] but the influence of greater charge also prevails. The μ-oxo exchange rates are also enhanced if terminal water molecules are bound to the Mn ion [76]. Given the apparent slow exchange rates of μ-oxo species it would seem unlikely that they represent the exchange of the slow site in PSII. It is interesting, however, that

Table 6
Water exchange rates for bridging oxo groups

Trivalent ion	Oxo exchange k_{ex} (s^{-1})[a]	$\Delta H^{\ddagger}$ (kJ mol^{-1})	Reference
Fe^{3+}/Fe^{3+} (μ-oxo) *ribonucleotide reductase*	8.3×10^{-4}	–	[114]
Cr^{3+}/Cr^{3+} (μ-OH)	1.1×10^{-5}	99.5	[83]
Rh^{3+}/Rh^{3+} (μ-OH)	Inert	–	[84,85]
Ru^{3+}/Ru^{4+} (μ-O)[a]	$\sim 6 \times 10^{-6}$	–	[115]
Mn^{3+}/Mn^{4+} (μ-O) (bpy)	5.4×10^{-4}	–	[76]
Mn^{3+}/Mn^{4+} (μ-O) (terpy)	2.5×10^{-4}	–	[76]
Mn^{3+}/Mn^{4+} (μ-O) (bpea)	3.2×10^{-4}	–	[76]
Mn^{4+}/Mn^{4+} (μ-O) (bpea)	$\leq 5.0 \times 10^{-5}$	–	[76]

[a] Oxo exchange is apparent at 60 °C but is not seen at room temperature [115,116].

DFT calculations indicate that the large activation barrier for oxo exchange [81] compares well with the 70–80 kJ mol^{-1} activation energy found for the slow substrate water exchange in PSII [38,45].

Terminal oxo exchange rates (i.e. M=O) have been kinetically determined in several porphyrin systems [89,90] and in only a few metal oxo ions [91,92]. The ligand exchange in these examples is considerably slower with rates of about 10^{-3} s^{-1}. Mechanistically the exchange appears to be dependent on the protonation state of the terminal oxo ligand as the rate determining step. In PSII oxo groups have been proposed as intermediates in the S-state cycle [37,93–95], but given the magnitude of the exchange rates they may well be too slow to accommodate the experimental rates [78]. Furthermore, the pH dependence for the two exchange rates in S_3 shows only a very modest effect [45] and given the pH titratability of the S-states [96,97] this would suggest proton concentrations are not a factor in the exchange of ^{18}O with at the substrate site. EXAFS investigations of Mn complexes also do not support a formal terminal oxo in the S_3 state [98].

5.8. Calcium

One Ca^{2+} ion is in close proximity to Mn ions of the OEC of PSII [52,68] and is coupled to the chemistry of water oxidation [99,100]. In terms of water binding the rate of -aqua exchange for Ca complexes is extremely fast due to a low surface charge density that corresponds to the large ionic radius of Ca (Table 4). The water exchange rate for $[Ca(H_2O)_6]^{2+}$ was estimated to be ~6–9 × 10^8 s^{-1} [65,101]. As the Ca^{2+} is an alkaline earth series ion there is no influence from ligand field stabilization energy and thus the aqua exchange associated with Ca might be predicted to be insensitive to the oxidation of surrounding Mn ions in the OEC. However, this is probably an over-simplification of the system as secondary effects may impinge upon the exchange mechanism as mentioned earlier in Section 5.

In PSII the Ca ion can be replaced functionally with a Sr ion [102–105]. The substitution of Sr ion makes for a useful comparison as Sr has an inherently larger ionic radius compared to Ca (Table 4). This effects a lengthening of bonds to the metal center and reduces hydration enthalpies, which combine to favor increased coordination geometry. Thus, substitution of Ca with Sr should be expected to lead to an increase in ligand exchange rates. Using a derivation of transition state theory to predict rate changes, $\log(k/k') \sim \Delta(\Delta G_{hydration}) \sim \Delta pK$, estimates of the exchange rates for Ca versus Sr were made [42]. The analysis was based on hydration enthalpy alone and made the assumption that hydration entropy would be similar for Ca and Sr. With the additional assumption that the difference in proton binding affinity between Sr and Ca in water is ΔpK ~0.4 [105], it was predicted that the aqua exchange rates would increase ~3-fold upon Sr substitution for Ca. DFT calculations also supported k_{ex} Sr > Ca [106,107]. In PSII the experimentally substituted Sr leads to an increase in the slow phase of exchange of about ~3-fold (Table 1). However, the large radius of Ca and even more so with Sr predict long M–O bonds and corresponding fast exchange. The aqua exchange rate for Sr^{2+} in Richen's book is given at ~1 × 10^9 s^{-1} [65]. There is a considerable discrepancy between a rate of 10^9 s^{-1} and the rates for PSII, despite the correlation with Sr^{2+} substitution. In order to rationalize an ^{18}O exchange mechanism in PSII that shows the large thermodynamic barrier (E_A of ~75 kJ mol^{-1}) and a relatively slow kinetic rate ($k_{ex} \sim 2$ s^{-1}) determined experimentally [38,45] a proposal was made that substrate water was a bridging Ca–O–Mn oxo bond [42]. This site would then be labilized upon Sr exchange and would in turn be significantly slower to exchange than a terminal water site. The computational experiments from Siegbahn and co-workers [81] predicted a barrier for Ca^{2+}–OH–Mn^{4+} to be ~44 kJ mol^{-1} and this was lower than for the equivalent Mn–OH–Mn arrangement, yet similar to exchange for water from a Mn^{4+} ion.

6. Summary and overview of exchange behavior

The exchange rates of aqua ions vary widely due to properties of the coordination. In PSII we have medium resolution structural information at 3.5 Å [52] and at 3.0 Å [68] that has been used to derive complete amino acid assignments and there is EXAFS information on the positioning of the Mn ions [69]. However, there are differences in the interpretation of the Mn coordination geometry within the 3.0–3.5 Å resolution limit and there is still no final consensus on the precise coordination of the Mn_4Ca cluster. For example the substrate binding sites have not been identified and the Mn coordination (6 vs. 5 coordinate) is an open question. Additionally, structural changes during the S-state transitions signaled from EXAFS [108,109] most likely play some role. From comparative ligand exchange assessment the aqua exchange rates are expected to show $Mn^{2+} > Mn^{3+} > Mn^{4+}$ and thus a slowing of ligand exchange is expected upon increasing oxidation states. In Table 2 the S-state dependent rates for PSII show slowing of the slow exchange water molecule $S_0 \rightarrow S_1$, and the fast site slows $S_1 \rightarrow S_2 \rightarrow S_3$. So the inference from this could be that the fast-exchanging and slow-exchanging substrate water sites undergo metal centered oxidation at these steps.

There has been extensive discussions in terms of accumulating charge on the catalytic Mn_4Ca cluster [110–112]. With the oxidation of the cluster and accumulation of oxidizing equivalents it is thermodynamically costly to bury charge in a protein of low dielectric so that it is likely that charge neutralization is important [113]. A measure of charge in PSII has been taken from electrochromic measurements and the general consensus is there is a +1 accumulation of charge during the $S_1 \rightarrow S_2$ transition, with the other S-state steps remaining more-or-less electroneutral while the charge reverses on the $S_3 \rightarrow S_0$ [111]. Thus based on the properties of the metal ions discussed above, the increase in the formal charge during the $S_1 \rightarrow S_2$ transition would ordinarily be expected to manifest a significant slowing down of aqua exchange on the oxidized Mn ion. It is possible that the fast-exchanging site is sensing this phenomenon as the fast exchange phase is unresolved in S_1 but seemly has slowed down upon attaining the S_2 state. However, the slow-exchanging site undergoes an unexpected

increase by 100× fold. A possible explanation is the protonation of a –OH group during the $S_1 \rightarrow S_2$ transition to form an $–OH_2$ aqua species. Ordinarily this would not be expected to coincide with a metal undergoing oxidation or accumulating charge as is occurring on the $S_1 \rightarrow S_2$ transition. Similarly, the magnitude of ligand *trans effects* are seemingly too small to accommodate this effect. Based on the E_A analysis of these sites [45] the energy difference for a $0.02 - 2\,s^{-1}$ increase in rate between the S_1 and S_2 states is $\sim 13\,kJ\,mol^{-1}$, and thus could be indicative of an overall structural rearrangement of the OEC involving the slow site, or possibly the formation of a particularly strong H-bonding interaction between the water molecules.

One of the clearest effects concerns the slow-exchange site which for the $S_2 \rightarrow S_3$ transition is unchanged in rate or activation barrier [39]. This substrate binding site based on what we have seen for other treatments such as the H/D isotope exchange does not change [45]. This means the Mn-substrate site does not even sense a change in H-bonds and would predict the same oxidation states in S_2 and S_3 and identical substrate composition.

Finally, if the two exchange rates are interpreted in terms of metal ligand exchange the formal intermediates associated with the ^{18}O exchange in our view most likely represent (1) a Mn–O–Ca species for the slow site and (2a) a $Mn–OH_x$ hydroxide or aqua group for the substrate in fast exchange. If the fast kinetic is interpreted as substrate entry rate of water into the OEC then (2b) the site of ^{18}O exchange must be in fast exchange but we obtain no mechanistic information into this rate determining process. However, given the striking changes in the slow phase there are some subtleties in the reaction sequence that will need to be rationalized.

7. Concluding remarks and future perspectives

The ^{18}O ligand exchange measurements of substrate water are governed by many complex mechanisms. The correlations of the inorganic model systems with the S-states provide valuable insights into the properties of the substrate binding sites throughout the reaction sequence. The results have both been used to support some mechanisms for water oxidation and to eliminate other proposals. Clearly there are several interpretations for these results and from the magnitude of the exchange rates and energy barriers experimentally determined; it is difficult to pin-point with certainty the Mn oxidation state or coordination geometry of the metal complex. However, the data overall always strongly support two independent water substrate binding sites that are non-equivalent in nature. In the future higher structural resolution coupled with computational analysis will undoubtedly be used to resolve the binding site question. Also it is likely future studies with model systems will provide a better basis set for comparison, particularly with the terminal aqua exchange rates. Our current research direction in the biological system involves probing water exchange kinetics with PSII mutants to pinpoint the substrate water onto the metal sits of the Mn_4Ca inorganic cluster that catalyses the remarkable water oxidation reaction.

Acknowledgments

This study was supported by the Australian Research Council DP0770149 and DP0450421. The authors wish to thank Dr. Ron Pace and Prof. Rob Stranger at ANU, and Gary Brudvig at Yale for valuable discussions.

References

[1] J. Raymond, D. Segre, Science 311 (2006) 1764.
[2] P. Ward, C. Labandeira, M. Laurin, R.A. Berner, Proc. Natl. Acad. Sci. U.S.A. 103 (2006) 16818.
[3] P. Joliot, G. Barbieri, R. Chabaud, Photochem. Photobiol. 10 (1969) 309.
[4] B. Kok, B. Forbush, M. McGloin, Photochem. Photobiol. 11 (1970) 457.
[5] J. Messinger, G. Renger, in: G. Renger (Ed.), Primary Processes of Photosynthesis: Basic Principles and Apparatus, Royal Society Chemistry, Cambridge, 2008.
[6] H. Dau, M. Haumann, Photosynth. Res. 2007, doi:10.1007/s11120.
[7] J. Barber, Biochem. Soc. Trans. 34 (2006) 619.
[8] W. Hillier, J. Messinger, in: T. Wydrzynski, K. Satoh (Eds.), Photosystem II: The Water:Plastoquinone Oxidoreductase in Photosynthesis, Springer, The Netherlands, 2005, p. 567.
[9] J.P. McEvoy, G.W. Brudvig, Chem. Rev. 106 (2006) 4455.
[10] T. Noguchi, M. Sugiura, Biochemistry 39 (2000) 10943.
[11] T. Noguchi, M. Sugiura, Biochemistry 41 (2002) 15706.
[12] G. Fischer, T. Wydrzynski, J. Phys. Chem. B 105 (2001) 12894.
[13] A. Cua, D.H. Stewart, M.J. Reifler, G.W. Brudvig, D.F. Bocian, J. Am. Chem. Soc. 122 (2000) 2069.
[14] H.A. Chu, M.T. Gardner, W. Hillier, G.T. Babcock, Photosynth. Res. 66 (2000) 57.
[15] H.-A. Chu, H. Sackett, G.T. Babcock, Biochemistry 39 (2000) 14371.
[16] Y. Kimura, A. Ishii, T. Yamanari, T.A. Ono, Biochemistry 44 (2005) 7613.
[17] F. Garczarek, L.S. Brown, J.K. Lanyi, K. Gerwert, Proc. Natl. Acad. Sci. U.S.A. 102 (2005) 3633.
[18] T. Wydrzynski, N. Zumbulyadis, P.G. Schmidt, Govindjee, Biochim. Biophys. Acta 408 (1975) 349.
[19] T.J. Wydrzynski, S.B. Marks, P.G. Schmidt, Govindjee, H.S. Gutowsky, Biochemistry 17 (1978) 2155.
[20] T. Wydrzynski, N. Zumbulyadis, P.G. Schmidt, H.S. Gutowsky, Govingjee, Proc. Natl. Acad. Sci. U.S.A. 73 (1976) 1196.
[21] P.R. Sharp, in: V.L. Pecoraro (Ed.), Manganese Redox Enzymes, VCH Publishers, New York, 1992, p. 177.
[22] T. Wydrzynski, G. Renger, Biochim. Biophys. Acta 851 (1986) 65.
[23] G.C. Dismukes, Y. Siderer, FEBS Lett. 121 (1980) 78.
[24] Ö. Hansson, L.-E. Andréasson, T. Vänngård, FEBS Lett. 195 (1986) 151.
[25] L.E. Andréasson, Ö. Hansson, K. Von Schenck, Biochim. Biophys. Acta 936 (1988) 351.
[26] M.C.W. Evans, J.H.A. Nugent, R.J. Ball, I. Muhiuddin, R.J. Pace, Biochemistry 43 (2004) 989.
[27] R.D. Britt, K.A. Campbell, J.M. Peloquin, M.L. Gilchrist, C.P. Aznar, M.M. Dicus, J. Robblee, J. Messinger, Biochim. Biophys. Acta (BBA)-Bioenerg. 1655 (2004) 158.
[28] K.A. Åhrling, M.C.W. Evans, J.H.A. Nugent, R.J. Ball, R.J. Pace, Biochemistry 45 (2006) 7069.
[29] H. Yamada, H. Mino, S. Itoh, Biochim. Biophys. Acta 1767 (2007) 197.
[30] W.F. Beck, J.C. Depaula, G.W. Brudvig, J. Am. Chem. Soc. 108 (1986) 4018.
[31] D.A. Force, D.W. Randall, G.A. Lorigan, K.L. Clemens, R.D. Britt, J. Am. Chem. Soc. 120 (1998) 13321.
[32] M.C.W. Evans, R.J. Ball, J.H.A. Nugent, FEBS Lett. 579 (2005) 3081.
[33] D.T. Richens, Chem. Rev. 105 (2005) 1961.
[34] R. Radmer, O. Ollinger, FEBS Lett. 110 (1980) 57.
[35] R. Radmer, O. Ollinger, FEBS Lett. 195 (1986) 285.
[36] K.P. Bader, G. Renger, G.H. Schmid, Photosynth. Res. 38 (1993) 355.
[37] J. Messinger, M. Badger, T. Wydrzynski, Proc. Natl. Acad. Sci. U.S.A. 92 (1995) 3209.

[38] W. Hillier, J. Messinger, T. Wydrzynski, Biochemistry 37 (1998) 16908.
[39] W. Hillier, T. Wydrzynski, Biochemistry 39 (2000) 4399.
[40] W. Hillier, G. Hendry, R.L. Burnap, T. Wydrzynski, J. Biol. Chem. 276 (2001) 46917.
[41] G. Hendry, T. Wydrzynski, Biochemistry 41 (2002) 13328.
[42] G. Hendry, T. Wydrzynski, Biochemistry 42 (2003) 6209.
[43] l. Konermann, J. Messinger, W. Hillier, in: J. Matysik, T.J. Aartsma (Eds.), Biophysical Techniques in Photosynthesis Research, vol. 2, Springer, The Netherlands, 2007.
[44] J. Messinger, W. Hillier, M. Badger, T. Wydrzynski, in: P. Mathis (Ed.), Photosynthesis: From Light to Biosphere, Kluwer Academic Publishers, Dordrecht, 1995, p. 283.
[45] W. Hillier, T. Wydrzynski, Phys. Chem. Chem. Phys. 6 (2004) 4882.
[46] T. Wydrzynski, W. Hillier, J. Messinger, Physiol. Plant. 96 (1996) 342.
[47] M. Borgnia, S. Nielsen, A. Engel, P. Agre, Annu. Rev. Biochem. 68 (1999) 425.
[48] M.L. Zeidel, S.V. Ambudkar, B.L. Smith, P. Agre, Biochemistry 31 (1992) 7436.
[49] G. Calamita, D. Ferri, P. Gena, G.E. Liquori, A. Cavalier, D. Thomas, M. Svelto, J. Biol. Chem. 280 (2005) 17149.
[50] W.G. Gregor, R.M. Cinco, H. Yu, V.K. Yachandra, R.D. Britt, Biochemistry 44 (2005) 8817.
[51] M. Petrek, M. Otyepka, P. Banas, P. Kosinova, J. Koca, J. Damborsky, BMC Bioinformatics 7 (2006).
[52] K.N. Ferreira, T. Iverson, K. Maghlaoui, J. Barber, S. Iwata, Science 303 (2004) 1831.
[53] J.W. Murray, J. Barber, J. Struct. Biol. 159 (2007) 228.
[54] S. Riistama, A. Puustinen, A. GarciaHorsman, S. Iwata, H. Michel, M. Wikström, Biochim. Biophys. Acta-Bioenerg. 1275 (1996) 1.
[55] M. Svensson-Ek, J. Abramson, G. Larsson, S. Tornroth, P. Brzezinski, S. Iwata, J. Mol. Biol. 321 (2002) 329.
[56] L. Salomonsson, A. Lee, R.B. Gennis, P. Brzezinski, Proc. Natl. Acad. Sci. U.S.A. 101 (2004) 11617.
[57] J. Cohen, K. Kim, P. King, M. Seibert, K. Schulten, Structure 13 (2005) 1321.
[58] J. Cohen, K. Kim, M. Posewitz, M.L. Ghirardi, K. Schulten, M. Seibert, P. King, Biochem. Soc. Trans. 33 (2005) 80.
[59] N. Uehlein, C. Lovisolo, F. Siefritz, R. Kaldenhoff, Nature 425 (2003) 734.
[60] D. Loqué, U. Ludewig, L.X. Yuan, N. von Wirén, Plant Physiol. 137 (2005) 671.
[61] F. Basolo, R.G. Pearson, The Mechanisms of Inorganic Reactions, Wiley, New York, 1958.
[62] F. Basolo, R.G. Pearson, The Mechanism of Inorganic Reactions; A Study of Metal Complexes in Solution, 2nd ed., Wiley, New York, 1967.
[63] C.H. Langford, H.B. Gray, Ligand Substitution Processes, Benjamin, New York, 1965.
[64] S.F. Lincoln, A.E. Merbach, Adv. Inorg. Chem. 42 (1995) 1.
[65] D.T. Richens, The Chemistry of Aqua Ions, John Wiley & Sons, Chichester, 1997.
[66] L. Helm, A.E. Merbach, Chem. Rev. 105 (2005) 1923.
[67] L. Helm, A.E. Merbach, Coord. Chem. Rev. 187 (1999) 151.
[68] B. Loll, J. Kern, W. Saenger, A. Zouni, J. Biesiadka, Nature 438 (2005) 1040.
[69] J. Yano, J. Kern, K. Sauer, M.J. Latimer, Y. Pushkar, J. Biesiadka, B. Loll, W. Saenger, J. Messinger, A. Zouni, V.K. Yachandra, Science 314 (2006) 821.
[70] R.J. Debus, Biochim. Biophys. Acta 1503 (2001) 164.
[71] A. Neubrand, F. Thaler, M. Korner, A. Zahl, C.D. Hubbard, R. van Eldik, J. Chem. Soc.-Dalton Trans. (2002) 957.
[72] Y. Ducommun, K.E. Newman, A.E. Merbach, Inorg. Chem. 19 (1980) 3696.
[73] L.V. Kulik, B. Epel, W. Lubitz, J. Messinger, J. Am. Chem. Soc. 127 (2005) 2392.
[74] L.V. Kulik, B. Epel, W. Lubitz, J. Messinger, J. Am. Chem. Soc., in press.
[75] D. Kuzek, R.J. Pace, Biochim. Biophys. Acta-Bioenerg. 1503 (2001) 123.
[76] R. Tagore, H.Y. Chen, R.H. Crabtree, G.W. Brudvig, J. Am. Chem. Soc. 128 (2006) 9457.
[77] R. Tagore, R.H. Crabtree, G.W. Brudvig, Inorg. Chem. 46 (2007) 2193.
[78] W. Hillier, T. Wydrzynski, Biochim. Biophys. Acta-Bioenerg. 1503 (2001) 197.
[79] F.P. Rotzinger, Chem. Rev. 105 (2005) 2003.
[80] F.P. Rotzinger, J. Am. Chem. Soc. 119 (1997) 5230.
[81] M. Lundberg, M.R.A. Blomberg, P.E.M. Siegbahn, Theor. Chem. Acc. 110 (2003) 130.
[82] J.P. Hunt, Coord. Chem. Rev. 7 (1971) 1.
[83] S.J. Crimp, L. Spiccia, H.R. Krouse, T.W. Swaddle, Inorg. Chem. 33 (1994) 465.
[84] A. Drljaca, L. Spiccia, H.R. Krouse, T.W. Swaddle, Inorg. Chem. 35 (1996) 985.
[85] A. Drljaca, A. Zahl, R. van Eldik, Inorg. Chem. 37 (1998) 3948.
[86] V.K. Yachandra, K. Sauer, M.P. Klein, Chem. Rev. 96 (1996) 2927.
[87] S.R. Cooper, M. Calvin, J. Am. Chem. Soc. 99 (1977) 6623.
[88] J.E. Sheats, R.S. Czernuszewicz, G.C. Dismukes, A.L. Rheingold, V. Petrouleas, J. Stubbe, W.H. Armstrong, R.H. Beer, S.J. Lippard, J. Am. Chem. Soc. 109 (1987) 1435.
[89] S. Hashimoto, Y. Tatsuno, T. Kitagawa, Proc. Natl. Acad. Sci. U.S.A. 83 (1986) 2417.
[90] J.T. Groves, J.B. Lee, S.S. Marla, J. Am. Chem. Soc. 119 (1997) 6269.
[91] M.D. Johnson, R.K. Murmann, Inorg. Chem. 22 (1983) 1068.
[92] R.L. Thompson, S.K. Lee, S.J. Geib, N.J. Cooper, Inorg. Chem. 32 (1993) 6067.
[93] C.W. Hoganson, N. Lydakis-Simantiris, X.-S. Tang, C. Tommos, K. Warncke, G.T. Babcock, B.A. Diner, J. McCracken, S. Styring, Photosynth. Res. 46 (1995) 177.
[94] H. Dau, L. Iuzzolino, J. Dittmer, Biochim. Biophys. Acta-Bioenerg. 1503 (2001) 24.
[95] J.S. Vrettos, J. Limburg, G.W. Brudvig, Biochim. Biophys. Acta-Bioenerg. 1503 (2001) 229.
[96] G. Bernat, F. Morvaridi, Y. Feyziyev, S. Styring, Biochemistry 41 (2002) 5830.
[97] H. Suzuki, M. Sugiura, T. Noguchi, Biochemistry 44 (2005) 1708.
[98] T.C. Weng, W.Y. Hsieh, E.S. Uffelman, S.W. Gordon-Wylie, T.J. Collins, V.L. Pecoraro, J.E. Penner-Hahn, J. Am. Chem. Soc. 126 (2004) 8070.
[99] H.J. van Gorkom, C.F. Yocum, in: T.J. Wydrzynski, K. Satoh (Eds.), Photosystem II: The Water:Plastoquinone Oxidoreductase in Photosynthesis, Springer, The Netherlands, 2005, p. 307.
[100] H. Suzuki, Y. Taguchi, M. Sugiura, A. Boussac, T. Noguchi, Biochemistry 45 (2006) 13454.
[101] G. Atkinson, M.M. Emara, R. Fernande, J. Phys. Chem. 78 (1974) 1913.
[102] D.F. Ghanotakis, G.T. Babcock, C.F. Yocum, FEBS Lett. 167 (1984) 127.
[103] A. Boussac, A.W. Rutherford, Biochemistry 27 (1988) 3476.
[104] T.-A. Ono, Y. Inoue, FEBS Lett. 227 (1988) 147.
[105] J.S. Vrettos, D.A. Stone, G.W. Brudvig, Biochemistry 40 (2001) 7937.
[106] D.J. Harris, J.P. Brodholt, D.M. Sherman, J. Phys. Chem. B 107 (2003) 9056.
[107] M.M. Naor, K. Van Nostrand, C. Dellago, Chem. Phys. Lett. 369 (2003) 159.
[108] V.K. Yachandra, in: T.J. Wydrzynski, K. Satoh (Eds.), Photosystem II: The Water:Plastoquinone Oxidoreductase in Photosynthesis, Springer, The Netherlands, 2005, p. 235.
[109] M. Haumann, C. Muller, P. Liebisch, L. Iuzzolino, J. Dittmer, M. Grabolle, T. Neisius, W. Meyer-Klaucke, H. Dau, Biochemistry 44 (2005) 1894.
[110] C. Tommos, G.T. Babcock, Acc. Chem. Res. 31 (1998) 18.
[111] E. Schlodder, H.T. Witt, J. Biol. Chem. 274 (1999) 30387.
[112] W. Junge, M. Haumann, R. Ahlbrink, A. Mulkidjanian, J. Clausen, Philos. Trans. Roy. Soc. B 357 (2002) 1407.
[113] P.R. Rich, in: D.S. Bendall (Ed.), Protein Electron Transfer, BIOS Scientific Publishers, Oxford, 1996, p. 217.
[114] B.M. Sjöberg, T.M. Loehr, J. Sanders-Loehr, Biochemistry 21 (1982) 96.
[115] J.K. Hurst, J.Z. Zhou, Y.B. Lei, Inorg. Chem. 31 (1992) 1010.
[116] H. Yamada, J.K. Hurst, J. Am. Chem. Soc. 122 (2000) 5303.